ISBN: 978-3-95450-232-5 ISSN: 2673-7000 doi:10.18429/JACoW-NAPAC2022-FRXD4

SUPPRESSING THE MICROBUNCHING INSTABILITY AT ATF USING LASER ASSISTED BUNCH COMPRESSION*

Q. R. Marksteiner†, P. M. Anisimov, B. E. Carlsten, G. A. Latour, E. I. Simakov, H. Xu
Los Alamos National Laboratory, Los Alamos, NM, USA

Abstract

The microbunching instability in linear accelerators can significantly increase the energy spread of an electron beam. The instability can be suppressed by artificially increasing the random energy spread of an electron beam, but this leads to unacceptably high energy spreads for future XFEL systems. One possibility of suppressing this instability is to use laser assisted bunch compression (LABC) instead of the second chicane in an XFEL system, thereby eliminating the cascaded chicane effect that magnifies the microbunching instability. An experiment is proposed at ATF to test this concept, and numerical simulations of the experiment are shown.

INTRODUCTION

There are several reasons why the eSASE [1] and LABC [2] schemes are promising and are being considered for future, more affordable Xray free electron lasers, including the fact that they can reduce the effects of CSR, ISR, and undulator wakes [3]. One of the most important differences of an eSASE or LABC accelerator compared with a conventional accelerator is that these accelerators reduce the effects of the microbunching instability (MBI) [4]. Here we propose an experiment where an electron beam is compressed to similar amounts with 2 bulk chicanes and with the LABC scheme, in order to verify that this technique can supress the MBI.

The Accelerator Test Facility (ATF) at Brookhaven National Laboratory (BNL) is an ideal location for experimentally verifying if the proposed compression architecture can suppress the MBI [5].

One of the most complicated aspects of our planned experiment is the existence of the dogleg at ATF. If we are not careful, the dogleg can modify the longitudinal current profile of the electron bunch, and can alter the results of our experiment. By carefully tuning the quads in the dogleg, the dispersive properties can be eliminated. We will show with simulation that the proposed compression architecture can meet its MBI suppression goal. The ATF beamline as well as the laser modulator and small chicane needed for the MBI suppression experiment are modeled in the numerical ELEctron Generation ANd Tracking (ELEGANT) code [6].

In Fig. 1, we show the predicted microbuncing gain of our experiment, for both the bulk compression and the LABC case. The idea is that we need to eliminate dispersion from the dogleg at wavelengths that are relevant to the microbunching gain, so that MBI will be preserved. In the following, we will discuss three issues that arose when trying to set up the beamline simulation to transport an electron bunch while also preserving the longitudinal structure we wish to analyze. Further, we provide matching optics parameters for bunches with two different energy spreads.

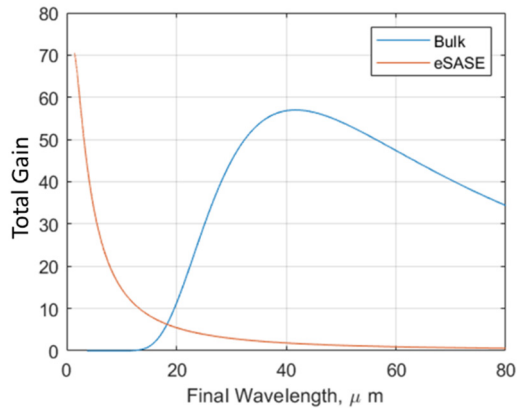

Figure 1: Predicted microbunching gain for the proposed eSASE and bulk compression schemes at ATF.

MINIMIZING DISPERSION

A schematic of the relevant optics that will be modelled is shown in Fig. 2. The dogleg must be tuned such that the amount of dispersion introduced to the bunch is minimized. Particles with varying momenta will be deflected differently by the two bending magnets that constitute the dogleg, i.e. higher momentum particles will be bent through a smaller angle and lower momentum particles through a larger angle. In addition, some particles will have a different path length through the dogleg than the ideal particle. This path length difference will result in particles arriving at the end of the dogleg at different times relative to their neighbors and the mismatch in arrival times will smear the longitudinal structure of the beam.

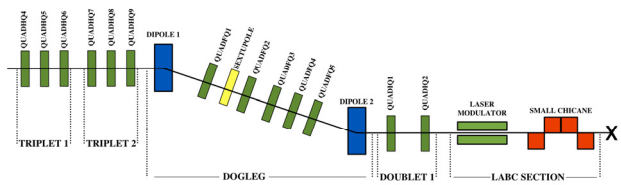

Figure 2: Drawing of the ATF beamline section that we model in ELEGANT. The beam propagates towards the right through the beamline.

In order to preserve the longitudinal structure of the beam, the matching optics in the dogleg need to be tuned such that the difference in path length, l, between particles of differing momenta is zero, i.e. $\Delta l \equiv 0$ between the

* We gratefully acknowledge the support of the US Department of Energy through the LANL LDRD program.
† qrm@lanl.gov

ISBN: 978-3-95450-232-5 ISSN: 2673-7000 doi:10.18429/JACoW-NAPAC2022-FRXD4

points $s = 0$ and $s = s_1$ independent of the momentum spread of the particles. Because the dogleg at ATF contains only two bending magnets, the difference in path length of the particles cannot be made zero. To make the particle path length difference through the dogleg as small as possible we utilized the optimization features integrated in the ELEGANT code to minimize the R_{51}, R_{52}, and R_{56} transfer matrix elements of the beamline. These three elements describe how a particle's z-coordinate changes from the beginning to end of the beamline based on its x- and x'-coordinates and momentum spread, respectively.

The optimization of the dogleg was done utilizing all available quadrupoles: the triplet before the dogleg, the quadrupoles in between the bending magnets, and the doublet after the dogleg. We set the optimization parameters listed in Table 1. These parameters had an upper limit so that ELEGANT had flexibility in converging to a solution. A small R_{56} for the dogleg was deemed acceptable because the R_{56} of the second small magnetic chicane could be decreased to compensate. Hence, the weight for the R_{56} constraint was set to 0.5.

Table 1: Optimization Parameters

Optimization Term	Value	Weight
Sx	≤ 50e-6 m	1.0
Sy	≤ 50e-6 m	1.0
Sx'	≤ 1.0	1.0
Sy'	≤ 1.0	1.0
R51^2	< 0.01	1.0
R52^2	< 0.01 m	1.0
R56^2	≤ 0.2 m	0.5

After optimization, the dogleg had very low dispersion values: R_{51}=0.09953 m, R_{52}=-0.09525, and R_{56}=-0.2757 m. In this optimization the bunch length increases from its initial rms size of 500 µm by just 200 nm, or just 0.04% of the initial bunch length. This is low enough so that the microbunching instability will not be suppressed.

The transverse phase space distribution which results from these optimized matching optics is shown in Fig. 3. The bunch has an rms size of about 25 µm in both x and y, 0.7 mrad in x' and 0.3 mrad in the y' coordinate.

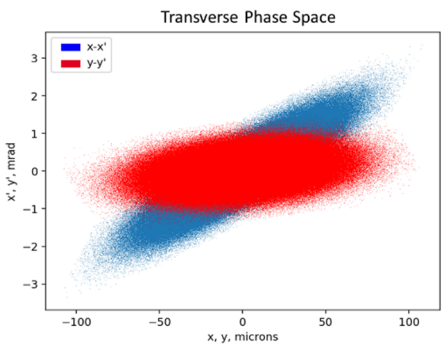

Figure 3: Transverse phase space of the bunch at the entrance of the laser modulator.

In order to test if the beam would modulate properly after the dogleg, a laser modulator was added into the ELEGANT simulation. The modulator had the properties of the RUBICON modulator at ATF [7]: total length 0.55 m, peak field 0.62 Tesla, 11 periods, and a laser wavelength of 9.2 µm. The peak power of the laser modulator element is calculated with the equation for electron energy modulation amplitude for electrons interacting with a resonant laser field [2]:

$$\Delta\gamma = \sqrt{\frac{P_L}{P_0}}\, 2K_m N_m \lambda_m [J_0(\tfrac{\xi}{2}) - J_1(\tfrac{\xi}{2})]/\gamma\omega_0,$$

where P_L is the peak laser power, $P_0 = I_A mc^2/e \approx 8.7$GW, $N_m \leq 0.05\gamma/\Delta\gamma_m$ is the number of undulator period of the modulator, $\xi = K_m^2/(2 + K_m^2)$, where K_m is the undulator parameter, ω_0 is the laser spot size, and λ_m is the modulator period. The modulation amplitude for this experiment is determined by the normalized modulation parameter, $A = \Delta\gamma/\sigma_\gamma = 12$. Figure 4 shows the modulated beam.

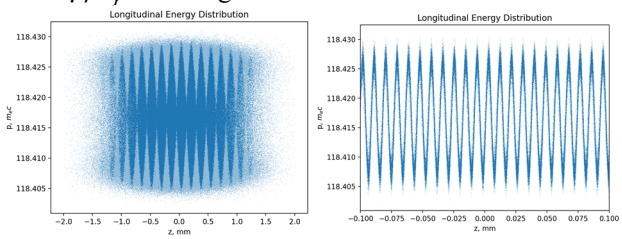

Figure 4: Longitudinal energy distribution of the modulated bunch (left), and zoomed in view of the same bunch (right).

INCREASED ENERGY SPREAD

In previous experiments at the ATF where laser modulation was used, such as the RUBICON and NOCIBUR experiments [7], simulations used a fractional momentum spread of 0.0015. However, in the simulation documented above, the fractional momentum spread was only 0.00001. Because a higher energy spread would itself suppress the MBI, the ATF will need to deliver a beam with as low an energy spread as possible. In the following, we study the effects of having this higher energy spread on the matching optics and laser modulation. The results will allow us to anticipate any potential issues that a higher energy spread could have on our experiment.

The bunch parameters in the ELEGANT simulation were updated to reflect the new energy spread. Likewise, the larger energy spread requires changing the peak power of the laser beam to achieve the required modulation parameter, $A = 12$. The required peak laser power is now 76.27062 MW.

With the same R_{56} as the previous optimization and the increased energy spread, the path length difference increases significantly. To compensate for the increased energy spread, the R_{56} of the beamline needs to be decreased. At the same time, the R_{51} and R_{52} or the beamline must be kept small to mitigate lengthening due to the particles' x and x'-coordinates.

ISBN: 978-3-95450-232-5 ISSN: 2673-7000 doi:10.18429/JACoW-NAPAC2022-FRXD4

Table 2: High Energy Spread Optimization Parameters

Optimization Term	Value	Weight
Sx	≤220e-6 m	1.0
Sy	≤220e-6 m	1.0
Sx'	≤ 0.0007	1.0
Sy'	≤ 0.0007	1.0
R51^2	< 0.05	1.0
R52^2	< 0.05 m	1.0
R56^2	≤ 0.016 m	0.8

In order to mitigate the larger spread in x' and the slope on the longitudinal energy distribution, we had to reoptimize the matching optics in the beamline. Further, there are a number of limitations placed on the bunch in the previous simulation that can be relaxed so that ELEGANT is able to achieve convergence in the upcoming optimization. Finally, ELEGANT had trouble converging to a solution with the available quadrupoles. The beamline was extended to include Triplet 1 shown in Fig. 2. In addition, the maximum allowable transverse size of the electron beam at the laser modulator was increased. This is not an issue, because the ~76 MW peak laser power from the previous simulation is far below the power capabilities of the BNL ATF CO2 laser.

Optimization with the higher energy spread, see Table 2, yields acceptable values for dispersion in the dogleg: R_{51}=0.450, R_{52}=0.517, and R_{56}=-0.0165. The bunch length from this simulation increases by just over 1 μm. This is an acceptable amount which will not disrupt the microbunching instability in the experiment.

The transverse phase space of the bunch at the entrance to the laser modulator has a boomerang shape in the $x - x'$ plane and has gained an odd wing shape in the $y - y'$ plane as well (see Fig. 5). However, because the rms transverse size of the bunch is only about 104 μm in x and 160 μm in y, and the spread in x' is only about 0.6 mrad, the strange shape of the transverse phase space does not really have an effect on our simulation. The bunch achieves all of our re-quirements, is stretched minimally by passage through the dogleg deflecting system, and it gains a satisfactory energy modulation after going through the laser mod-ulator. Figure 6 shows the modulation on the electron beam.

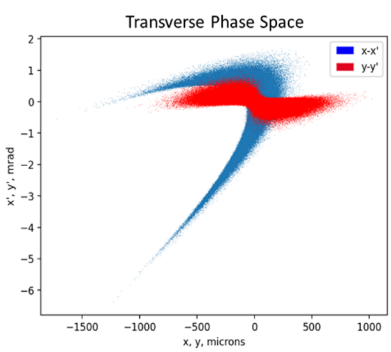

Figure 5: Transverse phase space of the higher energy spread bunch at the entrance of the laser modulator.

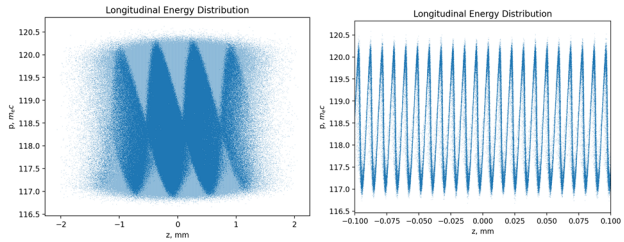

Figure 6: Longitudinal energy distribution of the higher energy spread bunch after exiting the laser modulator. The full bunch is shown on the left and a zoomed in picture on the right.

CONCLUSION

We have shown with ELEGANT simulations that the quadrupoles in the ATF dogleg can be tuned to minimize the dispersion. When the dispersion is minimized, the spreading out of electrons inside the dogleg is low enough so that the MBI is not suppressed. This will allow us to execute our proposed experiment at ATF. We will compress the electron beam with a two stage compression, and observe the MBI. Then we will compress with the LABC scheme, and observe the suppression of MBI.

AKNOWLEGEMENTS

Research presented in this report was supported by the Laboratory Directed Research and Development program of Los Alamos National Laboratory under project number 20200287ER.

REFERENCES

[1] A. A. Zholents, "Method of an enhanced self-amplified spontaneous emission for x-ray free electron lasers", *Phys. Rev. Spec. Top. Accel. Beams*, vol. 8, p. 040701, 2005. doi:10.1103/PhysRevSTAB.8.040701

[2] B. E. Carlsten, P. M. Anisimov, C. W. Barnes, Q. R. Marksteiner, R. R. Robles, and N. Yampolsky, "High-Brightness Beam Technology Development for a Future Dynamic Mesoscale Materials Science Capability", *Instruments*, vol. 3, p. 52, 2019. doi:10.3390/instruments3040052

[3] K. L. F. Bane and G. V. Stupakov, "Resistive Wall Wakefield in the LCLS Undulator", in *Proc. PAC'05*, Knoxville, TN, USA, May 2005, paper RPPE057, pp. 3390-3392. https://jacow.org/p05/papers/RPPE057.pdf

[4] Z. Huang *et al.*, "Suppression of microbunching instability in the Linac Coherent Light Source", *Phys. Rev. Spec. Top. Accel. Beams*, vol. 7, p. 074401, 2004. doi:10.1103/PhysRevSTAB.7.074401

[5] Accelerator Test Facility, https://www.bnl.com/atf

[6] M. Borland, "ELEGANT: A flexible SDDS-compliant code for accelerator simulation", Argonne National Laboratory, Lemont, IL, USA, Tech. Rep. ANL/APS/LS-287, 2005. doi:10.2172/761286

[7] N. S. Sudar, "Interactions of pre-bunched relativistic electron beams and electromagnetic waves in strongly tapered undulators," Ph.D. thesis, University of California, Los Angeles, CA, USA, 2019.